

B. Muth & P. Eberhard

Institute B of Mechanics, University of Stuttgart, Germany

[muth/eberhard]@mechb.uni-stuttgart.de

S. Luding

Technische Universiteit Delft, DelftChemTech, Particle Technology, The Netherlands

s.luding@tnw.tudelft.nl

ABSTRACT: In this paper different models for the simulation of granular material are investigated. Due to the fact, that a detailed simulation considering also complex shapes or the deformability of every single particle is very time consuming, methods from Molecular Dynamics are combined with methods from Multibody Systems, so that it is possible to determine the motion of many differently shaped bodies. Here, particles are modeled as rigid bodies, where the elasticity is described by means of elastic contact forces. The particles considered are convex or non-convex three-dimensional polyhedra.

1 INTRODUCTION

One goal of this work is the determination of the dynamical behavior of large systems, containing many differently shaped bodies. Of special interest are systems like hauling engines, shaking machines, filling constructions, etc., where a large number of solid bodies has to be investigated.

For the calculation of dynamical systems many different approaches exist. Bodies can be either treated as perfectly rigid objects, as non deformable objects with (small) overlaps at the contacts, or as deformable bodies with a peculiar contact dynamics. In the following we use the second approach, while the third one is currently under investigation.

In order to describe the interactions between different bodies, models from Molecular Dynamics (MD) are used here. These interactions depend on macroscopic measurable properties of the materials. Constitutive force laws are applied here to solid bodies, that are three dimensional and either spherical or of general polygonal shape.

2 MULTIBODY SYSTEMS

The systems considered here consist of free bodies in space. Such a system holds six degrees of freedom for each body, three translational \mathbf{y}_{Ti} and three rotational ones, \mathbf{y}_{Ri} . For the rotational degrees of freedom, e.g. Kardan-angles can be taken into account. All degrees of freedom can be summarized in a vector $\mathbf{y} = [\mathbf{y}_T \ \mathbf{y}_R]^T$ of generalized coordinates. Here, the bodies are only interdependent due to contact forces

and the equations of motion can be formulated without further constraints or joints for each body separately,

$$m_i \mathbf{H}_{Ti} \ddot{\mathbf{y}}_{Ti} = \mathbf{f}_i^e,$$

$$\mathbf{I}_i \mathbf{H}_{Ri} \ddot{\mathbf{y}}_{Ri} + \mathbf{I}_i \dot{\mathbf{H}}_{Ri} \dot{\mathbf{y}}_{Ri} + \boldsymbol{\omega}_i \times \mathbf{I}_i \boldsymbol{\omega}_i = \mathbf{l}_i^e. \quad (1)$$

Here, \mathbf{H}_{Ti} and \mathbf{H}_{Ri} are the Jacobian matrices of translation and rotation, respectively. Since the translational degrees of freedom are independent, \mathbf{H}_{Ti} equals the 3×3 identity matrix, whereas \mathbf{H}_{Ri} equals

$$\mathbf{H}_{Ri} = \begin{bmatrix} 1 & 0 & \sin \beta \\ 0 & \cos \alpha & -\sin \alpha \cos \beta \\ 0 & \sin \alpha & \cos \alpha \cos \beta \end{bmatrix}, \quad (2)$$

see (Schiehlen & Eberhard 2004), and $\dot{\mathbf{H}}_{Ri}$ is the time derivative of that Jacobian matrix. The mass of each body and its inertia tensor are denominated by m_i and \mathbf{I}_i , respectively. The rotational velocity is $\boldsymbol{\omega}_i = \mathbf{H}_{Ri} \dot{\mathbf{y}}_{Ri}$. Finally, \mathbf{f}_i^e and \mathbf{l}_i^e of Equation (1) are the forces and torques, that are acting on each body due to gravity and contact.

3 NEIGHBORHOOD SEARCH

For a system consisting of n bodies, the required calculation operations for collision detection will usually be of order $O(n^2)$, causing great computational effort. However, there exist special neighborhood search algorithms, so that a reduction of the computational effort down to the order $O(n)$ can be

achieved, (Allen & Tildesley 1989). The neighborhood search method we want to introduce here, the Linked Linear List (LLL), is described e.g. in (Schinner 1999). Every body whose bounding box is colliding with the bounding box of another particle is considered to be a neighbor of this body. Therefore, in a first step, bounding boxes are laid around each particle, see Figure 1, that are sized in such a way, that each particle fits exactly in its box. The edges of each bounding box are aligned with the coordinate axes. In a next step the bounding boxes are projected separately onto the system axes. The projection onto the x -axis is shown in Figure 1. In the following, only the order of the beginnings and endings of the projections of the bounding boxes along the axes is of interest. These beginnings and endings are identified here by a negative and positive value, respectively. These sequences are stored in lists with length of twice the number of particles in the system. If there is the beginning, ending, or both, of another particle in between the beginning and ending of a particular body, then there is an overlap of the projections of the bounding boxes of both particles along this axis. A collision of two bounding boxes exists only for an overlap of these projections along all axes. Although these lists have to be updated for each time step, the necessary calculation time is proportional to the number of particles in the system, corresponding to sorting an already nearly sorted list. The occurring changes are usually permutations only. If the order of the beginnings and endings does not have to be changed, the collision status of the particles also will remain unchanged. If a collision along an axis has to be removed, or if there is a new collision between two particles along an axis, the collision information along the other axes is essential and has to be compared, (Muth, Müller, Eberhard & Luding 2004).

The bodies, whose bounding boxes collide along all system axes, are called neighbors here. Each neighboring body-pair is now stored within a new list, called the LLL and checked further in the actual collision detection.

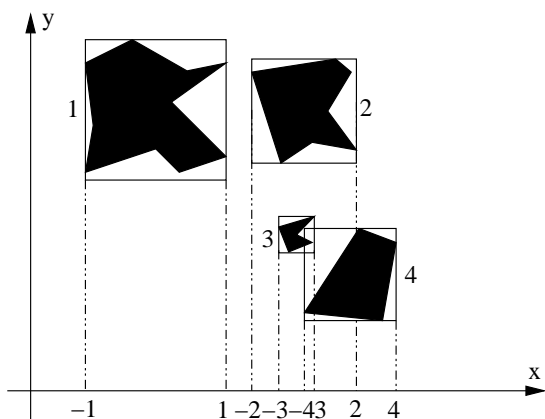


Figure 1. Bounding box projected onto the x -axis.

4 COLLISION DETECTION

As soon as neighboring body pairs are identified, the even more time consuming collision detection can be carried out. For body-pairs that are stored in the LLL, it is necessary to check, whether and which surface points are located inside another body. That means, for each neighboring body pair (e.g. body pair 3 and 4 in Figure 1) it has to be checked, whether vertices of polyhedron 3 lie within 4 and vice versa. In order to check, whether a point P is positioned within another body, e.g. the star-shaped body of Figure 2, a long ray originating from the observed point is created, and the intersections of this ray with the surface of the body are counted, (O'Rourke 1998).

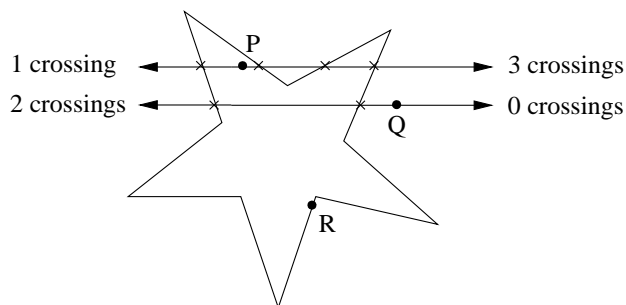


Figure 2. Collision detection for a planar example showing two possible rays for points P and Q .

Point P is inside the other body, if the number of intersections with the surface of the other body is odd for all possible rays. Equivalently, point Q is outside the other body, if the number of intersections is even for all rays from this point. In order to check that, the ray has to be tested against all separate surface parts of the body. By controlling, whether an intersection point of the ray with a surface plane lies on the surface of the body, the distance between the observed point and the surface is computed. If the distance between the observed point and the surface of the other body equals zero, then point R is positioned directly on the surface of the body, (O'Rourke 1998). These considerations have to be taken into account for each surface point of both neighboring bodies.

5 CONTACT FORCE

Since the investigated bodies here are solids, interactions between bodies are due to measurable properties of the bodies and their material such as viscosity, elasticity, frictional properties, and so on. These interactions are leading to contact forces, whose calculation is done following straight forward ideas from MD. They can be divided into normal and tangential contact forces. For the normal direction a penalty-formulation is used, i.e. overlaps between the bodies are accepted, and the magnitude of the contact force is dependent on this overlap. The contact forces are then calculated by means of the Calvin-Voigt model, (Lankarani & Nikravesh 1994), consisting of an elastic and a viscous part. The elastic part is proportional to the overlap of the two bodies. The abso-

lute value of the contact force is larger than the elastic part since the total value of the contact force could then become negative for negative relative velocity, and it therefore depends on the overlap as well. The contact force in normal direction is

$$\mathbf{f} = \underbrace{K\delta^n \mathbf{n}}_{\text{elastic force}} + \underbrace{K \frac{3(1-e^2)}{4\dot{\delta}_0} \delta^n \dot{\delta} \mathbf{n}}_{\text{viscous force}}. \quad (3)$$

Here, δ and $\dot{\delta}$ are the overlap between the two bodies and their relative velocity at the contact point, respectively. The exponent n can e.g. be 1, which leads to a linear contact law. The relative velocity at the beginning of the contact is denoted with $\dot{\delta}_0$ and e is a constant that corresponds to the coefficient of restitution when its value is close to one. That means, the damping coefficient d is here depending on the stiffness parameter K , and on the overlap between the bodies. This leads to a total relative kinetic energy during the contact of $\Delta T = \frac{1}{2} m_{\text{eff}} \dot{\delta}_0^2 (1-e^2)$. For a more detailed explanation of this see e.g. (Hunt & Grossley 1975; Lankarani & Nikravesh 1994).

For the implementation of the friction force, the simplest model would implement a velocity dependent tangential force with a cut-off at the Coulomb friction limit. Cundall and Strack proposed to use a tangential spring model where the tangential contact force is defined as

$$\mathbf{f}_t = -\frac{\boldsymbol{\xi}_t}{\|\boldsymbol{\xi}_t\|} \min(k\|\boldsymbol{\xi}_t\|, \mu \mathbf{f}_n). \quad (4)$$

That means the friction process is divided into a sticking and a sliding phase, and here the friction force acts opposite to a (small) tangential displacement that is allowed here also in the sticking phase due to elastic surface roughness. Therefore, in this approach the friction force is depending on the relative displacement. In Figure 3 the tangential plane is shown, where the occurring displacements and, therefore, the forces can be seen. Perpendicular to this plane is the normal direction with the normal contact force. Therefore, Figure 3 shows the tangential plane for a special normal contact force \mathbf{f}_N . The circle shows the border between the sticking and the sliding zone, with the radius being equivalent to $\mu \mathbf{f}_N$. Therefore, sticking occurs inside and sliding outside the circle. The beginning of the contact is at the origin of the coordinate system. In this example the line from 0 to 1 shows the tangential displacement $\boldsymbol{\xi}_{t1}$ of two bodies due to some acting forces. Point 1 is clearly within the sticking zone. Therefore, the contact force that has to be applied, \mathbf{F}_{t1} , is a sticking-force, its size being proportional to the distance between 0 and 1, see Figure 3. In a next time step, the tangential displacement may change, e.g., due to the impulse of another body in the system. Then the point that is in contact has moved

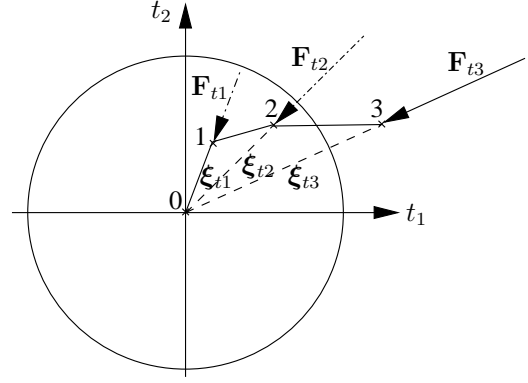


Figure 3. Cut of friction cone at actual normal force, parallel to the tangential plane.

again due to some forces and its projection onto the tangential plane is then, e.g., point 2. If this point is still within the circle, the sticking force is still proportional to the tangential displacement $\boldsymbol{\xi}_{t2}$ in its total direction and value, see \mathbf{F}_{t2} of Figure 3. That means, in each time step, the displacement $\boldsymbol{\xi}_t$ in tangential direction has to be re-calculated from the relative velocity and added up vectorially. The force is then applied in opposite direction of that total displacement. As soon as sliding occurs, e.g. in the timestep from point 2 to 3, the value of the friction force will be restricted to the sliding force. That means, its magnitude is restricted to $\mu_d \mathbf{f}_N$. The direction of this force still changes with each time step and will always be directed to the origin of the tangential system, i.e. the point of first contact.

If, in a later time step, when the contact still exists, the relative motion stops and changes its direction, a sticking force has to be applied to the bodies. By means of the conventional Cundall-Strack model, this is not possible, see (Brendel & Dippel 1998). If the elongation of $\boldsymbol{\xi}_t$ has been updated in each time step, after a long sliding phase it will take a long backwards motion in opposite direction to release this “spring”. Therefore, (Brendel & Dippel 1998) propose not to update the elongation of $\boldsymbol{\xi}_t$ during sliding, but to keep it constant, i.e., at the value that corresponds to the particular radius of the circle, until sticking occurs again. The solution for the contact force in a planar example is given in (Brendel & Dippel 1998), and is extended here to a spatial statement,

$$\mathbf{f}_t = -k_t \boldsymbol{\xi}_t, \quad (5)$$

$$\boldsymbol{\xi}_t = \int_{t_0}^t \mathbf{v}_t \Theta(\mu \|\mathbf{f}_n\| - k_t \|\boldsymbol{\xi}_t\|) dt', \quad (6)$$

where $\Theta(\bullet)$ is the Heaviside function. Therefore, an update of $\boldsymbol{\xi}_t$ will only be carried out for $\mu \|\mathbf{f}_n\| > k_t \|\boldsymbol{\xi}_t\|$.

6 EXAMPLE

In this example the advantage of the above friction model is shown. Contrary to models, where the friction force is detected by means of the relative velocity

between two bodies, here e.g. a block on an inclined plane can come to rest. Such an example is shown here, with a nonconvex block of volume $0.001m^3$. It has the density of $\rho = 2700 kg/m^3$, therefore its mass is $m = 2.7kg$. The angle of the inclined plane on which the block is located is $\alpha = 30^\circ$ and the critical value for the friction coefficient is $\mu = \tan(\alpha) \approx 0.57735$. Here, the block is located in its balanced state in normal direction. Tangentially to the plane, an initial velocity $v_0 = 5m/s$ is given to the block. So, the block is sliding upward first, until at a special time the relative velocity is zero. This time can be determined as $t = v_0 / (g \sin(\alpha) + \mu g \cos(\alpha))$. In the following, a simulation with a time step size of $\Delta t = 5e-6s$ is carried out for three different values of μ around the critical value. For this example, time t_1 at which the velocity of the block gets zero for $\mu_1 = 0.5$ is $t_1 \approx 0.546s$. For a friction coefficient of $\mu_2 = 0.58$, $t_2 \approx 0.508s$, and finally for $\mu_3 = 0.6$ we get $t_3 \approx 0.499s$. In Figure 4 the velocity of the block is shown over the time. As an inset, the assembly of the example, i.e. the nonconvex block on the plane is shown. The block is gliding upwards, while its velocity drops until it gets zero at a certain point. At this point, the block comes to rest. For $\mu_1 < \tan(\alpha)$, the velocity drops further, it changes its sign and gets negative, i.e., the block glides down the plane. A more detailed image of the scene is given in Figure 5. Here, points t_1 , t_2 , and t_3 , are specified, at which the velocity is zero. It can be seen clearly, that for all cases, the velocity decreases further for a short time, since the block moves downward during sticking. Then, after sticking is overridden, the velocity for the small friction coefficient decreases further. For μ_2 and μ_3 , the velocity rises until it gets zero and remains there.

7 CONCLUSIONS

In this paper we described different models that are used to obtain an efficient program for the simu-

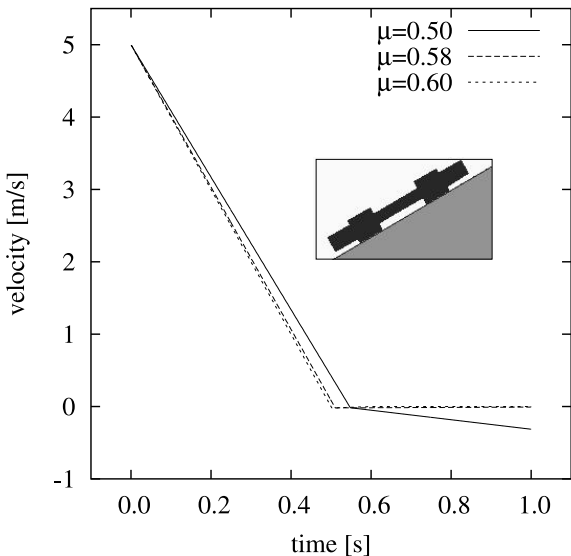


Figure 4. Velocity of the nonconvex block on an inclined plane for three different friction coefficients.

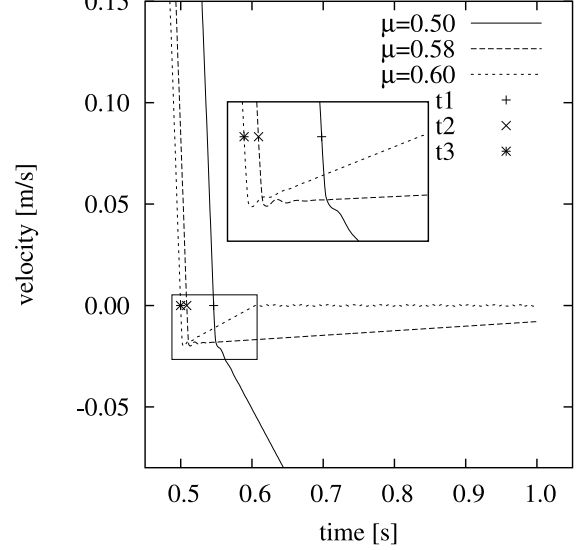


Figure 5. Zoomed depiction of the velocity of the block.

lation of granular media. The combination of ideas from MD and MBS makes it possible to simulate the dynamical behavior of large systems of differently shaped bodies efficiently. First, the equations of motion for arbitrary solid bodies are obtained. By means of a neighborhood search method, neighboring bodies are presorted such that the very time consuming collision detection only has to be accomplished for bodies that are positioned very close to each other. The contact forces are modeled by the Calvin-Voigt model in normal direction. We described the Cundall-Strack model in detail, which is used to model the frictional contact force here. We depicted results for three different friction coefficients and could show, that e.g. a block on an inclined plane can completely come to rest.

REFERENCES

- Allen, M.P. & Tildesley, D.J. 1989. *Computer Simulations of Liquids*. Oxford: Clarendon Press.
- Brendel, L. & Dippel, S. 1998. Lasting Contacts in Molecular Dynamics Simulations. In H. J. Herrmann, J.-P. Hovi and S. Luding (eds.), *Physics of Dry Granular Materials*, NATO ASI Series E 350: 313-318. Dordrecht: Kluwer.
- Cundall, P.A. & Strack, O.D.L. 1979. A Discrete Numerical Model for Granular Assemblies. *Geotechnique* 29(1): 47-65.
- Hunt, K.H. & Grossley, F.R.E. 1975. Coefficient of Restitution Interpreted as Damping in Vibroimpact. *ASME Journal of Applied Mechanics* 7: 440-445.
- Lankarani, H.M. & Nikravesh, P.E. 1994. Continuous Contact Force Models for Impact Analysis in Multibody Systems. *Nonlinear Dynamics* 5: 193-207.
- Muth, B.; Müller, M.-K.; Eberhard, P. and Luding, S. 2004. Contacts between Many Bodies. *Machine Dynamics Problems* 28(1): 101-114.
- O'Rourke, J. 1998. *Computational Geometry in C*, (2. edition). Cambridge: Cambridge University Press.
- Schiehlen, W. & Eberhard, P. 2004. *Technische Dynamik – Modelle für Regelung und Simulation* (in German). Stuttgart: Teubner.
- Schinner, A. 1999. Fast Algorithms for the Simulation of Polygonal Particles. *Granular Matter* 2(1): 35-43.